SISSA

Experimental determination of proton hardness factors at several irradiation facilities

View the article online for updates and enhancements.

IOP ebooks™

Bringing you innovative digital publishing with leading voices to create your essential collection of books in STEM research.

Start exploring the collection - download the first chapter of every title for free.

Experimental determination of proton hardness factors at several irradiation facilities

P. Allport,[a] F. Bögelspacher,[c] K. Bruce,[a] R. Canavan,[a] A. Dierlamm,[c] L. Gonella,[a] P. Knights,[a] I. Mateu,[b] M. Moll,[b] K. Nikolopoulos,[a,1] B. Phoenix,[a] T. Price,[a] L. Ram,[a] F. Ravotti,[b] C. Simpson-Allsop[a] and C. Wood[a]

[a] *University of Birmingham,*
  Birmingham, B15 2TT, U.K.

[b] *IRRAD Proton Facility,*
  CERN, CH-1211 Geneva 23, Switzerland

[c] *Institute of Experimental Particle Physics, Karlsruhe Institute of Technology,*
  Karlsruhe, D-76131, Germany

  E-mail: k.nikolopoulos@bham.ac.uk

ABSTRACT: The scheduled High Luminosity upgrade of the CERN Large Hadron Collider presents new challenges in terms of radiation hardness. As a consequence, campaigns to qualify the radiation hardness of detector sensors and components are undertaken worldwide. The effects of irradiation with beams of different particle species and energy, aiming to assess displacement damage in semiconductor devices, are communicated in terms of the equivalent 1 MeV neutron fluence, using the hardness factor for the conversion. In this work, the hardness factors for protons at three different kinetic energies have been measured by analysing the I–V and C–V characteristics of reverse biased diodes, pre- and post-irradiation. The sensors were irradiated at the MC40 Cyclotron of the University of Birmingham, the cyclotron at the Karlsruhe Institute of Technology, and the IRRAD proton facility at CERN, with the respective measured proton hardness factors being: 2.1 ± 0.5 for 24 MeV, 2.2 ± 0.4 for 23 MeV, and 0.62 ± 0.04 for 23 GeV. The hardness factors currently used in these three facilities are in agreement with the presented measurements.

---

[1]Corresponding author.

Contents

1 Introduction

The scheduled upgrade of the CERN Large Hadron Collider [1] to its High Luminosity phase (HL–LHC) in 2024 [2] presents new challenges in terms of detector radiation hardness [3, 4]. In irradiation facilities around the world, campaigns to qualify radiation hardness of detector sensors are undertaken. Standard 1 MeV neutron equivalent fluences are used for the purpose of inter-facility comparison and collaboration. The experimentally determined proton fluences at given energies are converted to the standardised fluences using the corresponding hardness factor. This factor is usually derived by evaluating the leakage current in the bulk of a silicon sensor; assuming that the measured leakage current is scaling with the non-ionizing energy loss (NIEL).

At the University of Birmingham, the MC40 cyclotron adopts a hardness factor value of 2.2 [5] for protons of 23 MeV. However, for beams of similar kinetic energy, facilities have obtained different values. For example, the Irradiation Center Karlsruhe has recorded a value of 2.05 ± 0.61 for 24 MeV protons, with a previously assumed value of 1.85 for 26 MeV protons [6]. Other studies have claimed similar values, such as 2.22 for 27 MeV protons [7]. Tabulated values from the RD50 Collaboration, which is concerned with the development of radiation hard semiconductor devices for high luminosity colliders [8], give a value of approximately 2.56 for 25 MeV protons [9]. For 23 GeV protons, a value of 0.62 has been measured at the IRRAD proton facility [7]. Due to these discrepancies, further study on the value of the hardness factor is required. Moreover, the large uncertainties of these measurements result to large uncertainties when the proton fluences are converted to the corresponding 1 MeV neutron equivalent fluences.

In this article the current-voltage (I–V) and capacitance-voltage (C–V) characteristics of reversed biased BPW34F photodiodes are analysed to obtain proton hardness factors for protons of three different kinetic energies. In the following the irradiation facilities are presented briefly in section 2, while the description of the measurements is given in section 3. The obtained results are presented in section 4, while a concluding discussion is given in section 5.

2 Irradiations

2.1 MC40 cyclotron

The MC40 cyclotron at the University of Birmingham is primarily used for the production of medical isotopes. However, it is regularly used for nuclear physics research and radiation damage studies. The configuration utilised for high intensity proton irradiations is shown in figure 1. The beam spot is a square of area $10 \times 10 \, \text{mm}^2$, and its position is calibrated before each irradiation session with gafchromic film. The sample is isolated from the environment using a temperature controlled chamber, which is is mounted on a XY-axis robotic scanning system controlled via LabView. The chamber temperature during irradiation is set to $-27°\text{C}$, this is selected to ensure that the sample temperature remains well below $0°\text{C}$, even when irradiated at the highest available dose rate in the facility, and thus there will be no significant contribution to thermal annealing. Further details for the irradiation facility are provided in ref. [10].

(a)   (b)

Figure 1. (a) The high intensity area of the MC40 cyclotron with the temperature controlled chamber. (b) The interior of the temperature controlled chamber, viewed from the side. The aluminium plate used to mount the diodes is visible on the right.

The irradiated sample consists of an aluminium plate with twelve slots for diodes, mounted in pairs, as shown in figure 2. In front of each pair of diodes, ^{57}Ni foils are installed and their activity after irradiation is used to estimate the delivered proton fluence. Inside the temperature controlled chamber, the sample and the foils, are placed behind a $350 \, \mu\text{m}$ thick sheet of aluminium to block possible low energy components of the beam. The energy of the proton beam when they reach the sample, is estimated using a Geant4-based [11, 12] simulation, as shown in figure 3.

2.2 IRRAD proton facility

The IRRAD proton facility at CERN utilises a primary proton beam with an energy of $23 \, \text{GeV}$, extracted from the proton synchrotron [13]. The facility employs the use of a remote controlled
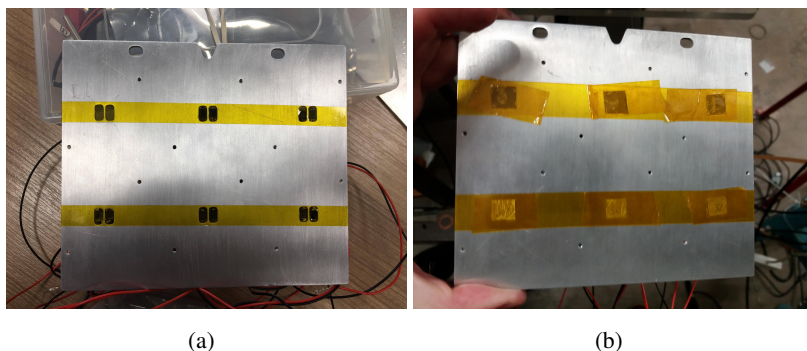
(a)   (b)

Figure 2. (a) Aluminium diode mount with attached diodes; and (b) the same mount following placement of ^{57}Ni foils for fluence measurements.
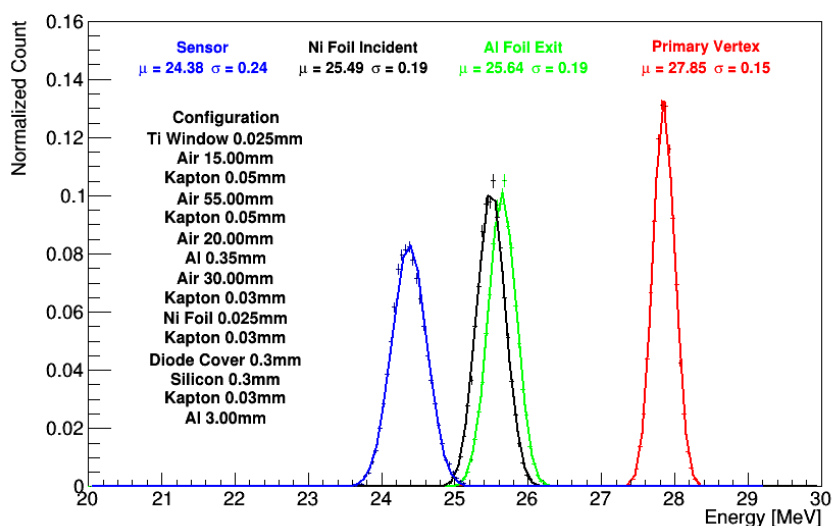

Figure 3. Geant4 simulation of the MC40 cyclotron beam-line showing the incident proton beam energy, the energy at the nickel foils, and the energy at the photodiodes.

stage to adjust the position of the sample, and an isolated box for humidity and temperature control down to approximately −20°C [14]. The proton fluence determination for IRRAD is performed with aluminium foils. Figure 4 shows an image of the IRRAD setup and the remote controllable tables, which can move in the transverse and azimuthal directions to align the sample with the beam. This setup also allows for beam scanning, which can be done automatically. Furthermore, there are three blocks of three tables along the beam line, each separated by thick blocks of concrete.

For this study, both BPW34F photodiodes and FZ pad diodes were irradiated to the same fluences for NIEL comparisons. Irradiations take place at room temperature, and given the dose rate on the samples no appreciable thermal annealing is expected to take place, in particular when compared to the thermal annealing applied during the analysis procedure, see section 3.1.
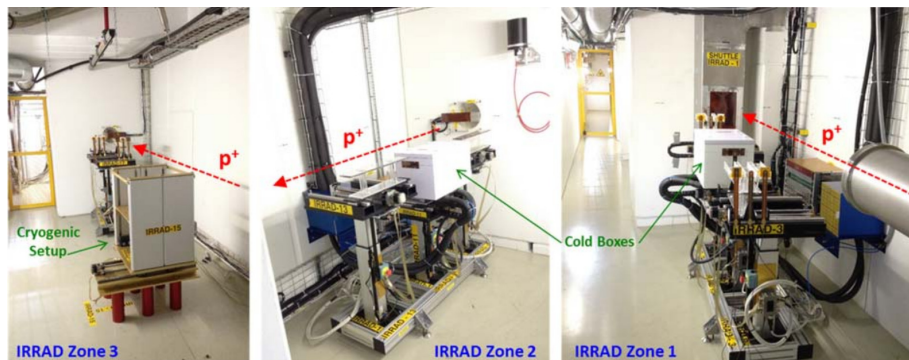
Figure 4. IRRAD proton facility experimental areas featuring three groups of remote-controlled tables installed along the proton beam path, from ref. [15].

2.3 Irradiation Center Karlsruhe

The Irradiation Center Karlsruhe [16] accesses a compact cyclotron operated by ZAG Zyklotron AG [17], a private-owned company specialising in radioisotopes production for medicine and engineering. The cyclotron accelerates protons to 25 MeV and for this study the energy of the protons at the sample was measured to be 23 MeV. The set-up utilised for irradiations is shown in figure 5. Similarly to the MC40 cyclotron and the IRRAD proton facility, the sample can be positioned within an isolation box for humidity and temperature control down to −30°C [16], and the fluences are calculated using ^{57}Ni foils.
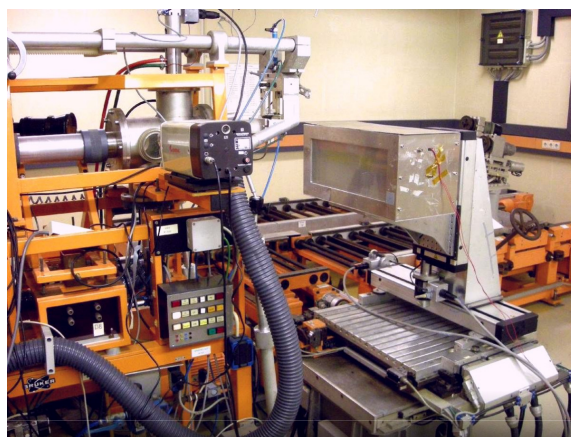

Figure 5. The Karlsruhe proton irradiation setup with the beam pipe visible on the left and the cold box on the right. During irradiation the box is moving to allow beam scanning over the whole area of interest.

3 Measurements

3.1 Thermal annealing procedure

Since the degree of thermal annealing significantly affects the post-irradiation leakage current of photodiodes, all diodes where thermally annealed for 80 minutes at 60°C in accordance with the

guidelines of the RD50 collaboration. This ensured that post-irradiation, all diodes possessed the same thermal history. The process itself utilised a pre-heated oven, monitored with a NiCr-NiAl thermocouple. For the MC40 cyclotron, due to the large number of diodes tested, thermal annealing took place in two sets, with half of the diodes in each set.

3.2 Maximum depletion voltage

To estimate the value of the voltage where maximum depletion is achieved, the diodes were placed inside an aluminium box for radiation shielding, as shown in figure 6, alongside a fan for air circulation. The system was then connected to a Wayne-Kerr 6500B Precision Impedance Analyser via a junction box and four coaxial cables for capacitance readings at 10 kHz; in accordance with RD50 guidelines. An external bias was supplied to the diodes by a Keithley 2410 Sourcemeter. The system was then trimmed to approximately zero capacitance with the diode unconnected before each set of data was taken.
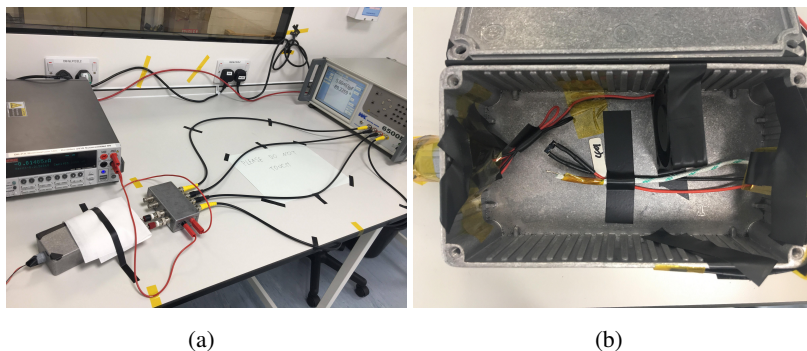

(a)   (b)

Figure 6. (a) C–V measurement set-up, with the Wayne-Kerr 6500B Precision Impedance Analyser, the Keithley 2410 Sourcemeter, and the aluminium box; (b) Internal view of the aluminium box.

For a p-n junction, before full depletion, the capacitance is inversely proportional to the square root of the voltage. Following full depletion, capacitance becomes independent of the voltage. Using this, it is possible to estimate the voltage at which a diode becomes fully depleted, referred to as the maximum depletion voltage. Figure 7 shows a plot of capacitance as a function of voltage in logarithmic scales. In region (1), the diode is not fully depleted, whilst in region (2), full depletion has been achieved. In the latter region, the gradient is not zero as the BPW34F diode does not contain a guard ring, and thus lateral depletion is still occurring. By fitting the two regions linearly, the maximum depletion voltage is estimated as the intercept of the two lines. This estimate was performed for every diode following irradiation and annealing.

3.3 Quantifying radiation damage

Figure 8 shows the experimental setup used for I–V measurements. Similarly to the capacitance measurements, the diodes were placed within an aluminium box alongside a fan. A Keithley 2410 source meter was used to apply a reverse bias across the diode, which was then measured and displayed the corresponding current. A NiCr-NiAl thermocouple was used to record the temperature within the box, being placed close to the diode to obtain an accurate reading of its temperature.
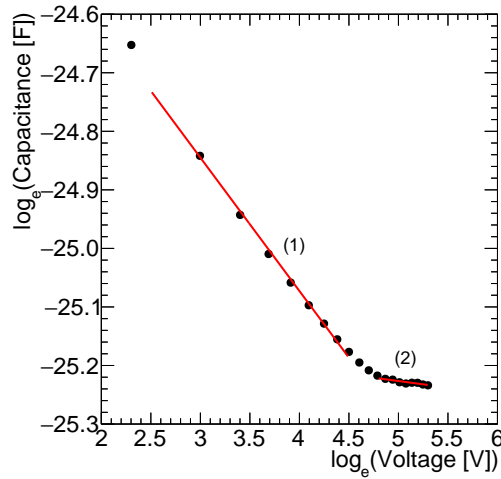
Figure 7. Capacitance as a function of reverse bias for a BPW34F photodiode irradiated to 4.33×10^{11} p/cm^2.
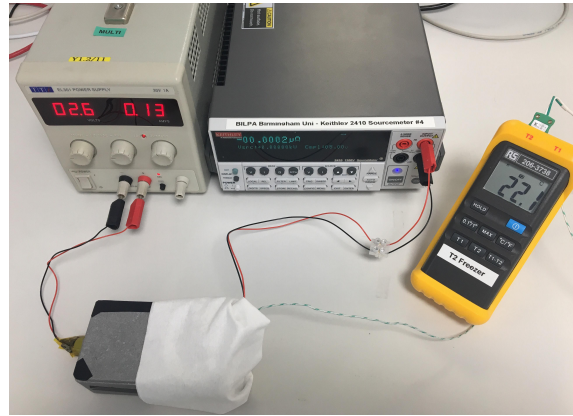

Figure 8. The setup utilised for I–V measurements.

Although the ambient temperature, T, during data taking did not deviate substantiall from 21°C, to minimise any effects due to the temperature dependence of the leakage current, all I–V curves were normalised to the reference temperature, T_R, of 21°C, following RD50 recommendations. The formula used is given in eq. (3.1), where E_a is the activation energy of silicon, which is closely related to the band gap energy of silicon, and all other symbols have their usual meanings.

$$I(T_R) = I(T) \left(\frac{T_R}{T}\right)^2 e^{-\frac{E_a}{2k_B}\left[\frac{1}{T_R} - \frac{1}{T}\right]} \tag{3.1}$$

Over the temperature range relevant for this study, E_a has a value of 1.21 eV [18]. Post-irradiation, the leakage current of the diodes increased proportionally to the incident fluence due to induced defects in the silicon [19]. Hence, the change in leakage current pre- and post- irradiation can be used as a measure of the degree of radiation damage. Assuming that the leakage current scaled with the NIEL irrespective of the particle species and energy, the change in leakage current can be used to determine the hardness factor.

3.4 Determination of hardness factors

The change in leakage current pre- and post- irradiation, ΔI, as a function of fluence, ϕ is:

$$\Delta I = \alpha l^2 w \phi \tag{3.2}$$

where α is the current related damage rate, l^2 is the active area of silicon, and w is the width of the depletion region. For BPW34F photodiodes, $l^2 = (0.265 \times 0.265) \, \text{cm}^2$ [20, 21] and $w = 300 \, \mu\text{m}$ [22]. From equation (3.2), and the NIEL scaling hypothesis, it follows that the hardness factor can be written as:

$$\kappa = \frac{\phi_{\text{neq}}}{\phi}, \tag{3.3}$$

where ϕ_{neq} is the 1 MeV neutron equivalent fluence. Combining equations. (3.2) and (3.3), the hardness factor can be obtained as:

$$\kappa = \frac{\alpha}{\alpha_{\text{neq}}}, \tag{3.4}$$

where α_{neq} is the current related damage rate for 1 MeV neutrons. In this study, $\alpha_{\text{neq}} = (3.99 \pm 0.03) \times 10^{-17} \, \text{Acm}^{-1}$ was used [19]. Thus, by comparing the diode leakage current pre- and post-irradiation as a function of fluence, the hardness factor of the incident beam is calculated.
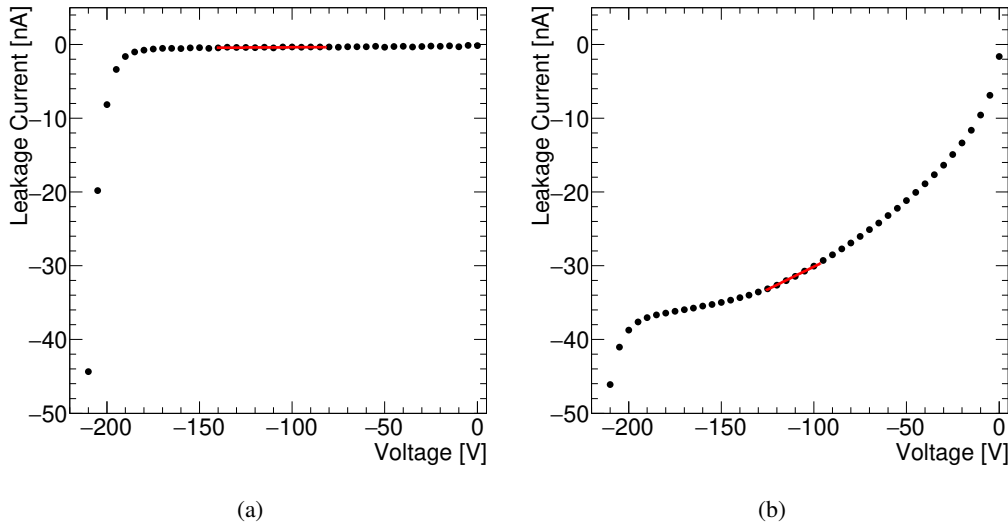

Figure 9. I–V curves fit with a first order polynomial. (a) Unirradiated diode; (b) Following irradiation at $(1.64 \pm 0.36) \times 10^{11} \text{pcm}^{-2}$ and thermal annealing.

Figure 9 shows I–V curves for the same diode pre- and post-irradiation and annealing. The data were fit with a first order polynomial centred at the minimum voltage value for which the depletion region is maximised, as determined from C–V measurements. The change in leakage current, evaluated at this voltage, was computed for each diode and plot as a function of fluence.

Finally, the range of validity of eq. (3.2) has been considered in a dedicated study at the MC40 cyclotron. As shown in figure 10, the change in leakage current is linear as a function of fluence up to fluences of approximately $10^{14} \, \text{pcm}^{-2}$. At low fluences, all charge carriers generated by the radiation-induced defects are transported to the electrodes and contribute fully to the leakage current
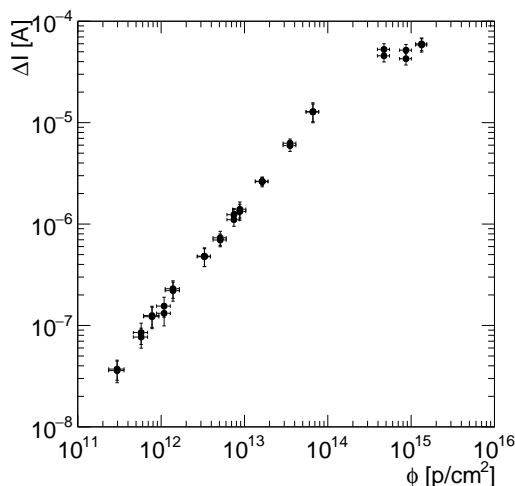
Figure 10. Change in leakage current as a function of fluence for the BPW34F diodes. The linearity of response up to approximately 10^{14}p/cm^2 is demonstrated.

(Shockley-Read-Hall mechanism). At high fluences the high defect concentration results to charge carriers getting trapped. As a result, these are not transported throughout the sensor, which results to the observed plateau of the change in leakage current versus fluence.

4 Results

The measured change in leakage current as a function of the fluence for BPW34F photodiodes, irradiated with 24 MeV protons at the MC40 cyclotron, are shown in figure 11(a). The data were fit with a straight line, which was required to pass through the origin. As there should be no change in leakage current, unless the diode is irradiated. Nevertheless, leaving the intercept free in the fit, did not significantly change the result. Using equations (3.2) and (3.4), a hardness factor value of $\kappa^{24\,\text{MeV}} = 2.11 \pm 0.49$ was determined.

The measured ΔI as a function of fluence for a collection of BPW34F and BPW34FS diodes irradiated with 23 MeV protons at the Irradiation Center Karlsruhe is presented in figure 11(b). For these data, the fit was not forced through zero, as the pre-irradiation state for each diode was not known. However, the change in leakage current between the pre- and post-irradiated case is of several orders of magnitude, and so the change in leakage current was approximated to the post-irradiated leakage current following thermal annealing. Furthermore, given the discussion in section 3.4, the highest fluence point of figure 11(b) was omitted from the fit. Applying equations (3.2) and (3.4) as before, a value of $\kappa^{23\,\text{MeV}} = 2.20 \pm 0.43$ was determined.

Figure 11(c) shows the change in leakage current as a function of fluence for BPW34F photodiodes irradiated with 23 GeV protons at the IRRAD proton facility. Again, the data were fit with a first order polynomial that was required to go through the origin. From this, a value of $\kappa^{23\,\text{GeV}} = 0.62 \pm 0.04$ was obtained. In figure 11(d) the corresponding results for FZ pad diodes, irradiated to the same fluences at IRRAD, are presented. A value of $\kappa'^{23\,\text{GeV}} = 0.62 \pm 0.03$ was obtained from these data.
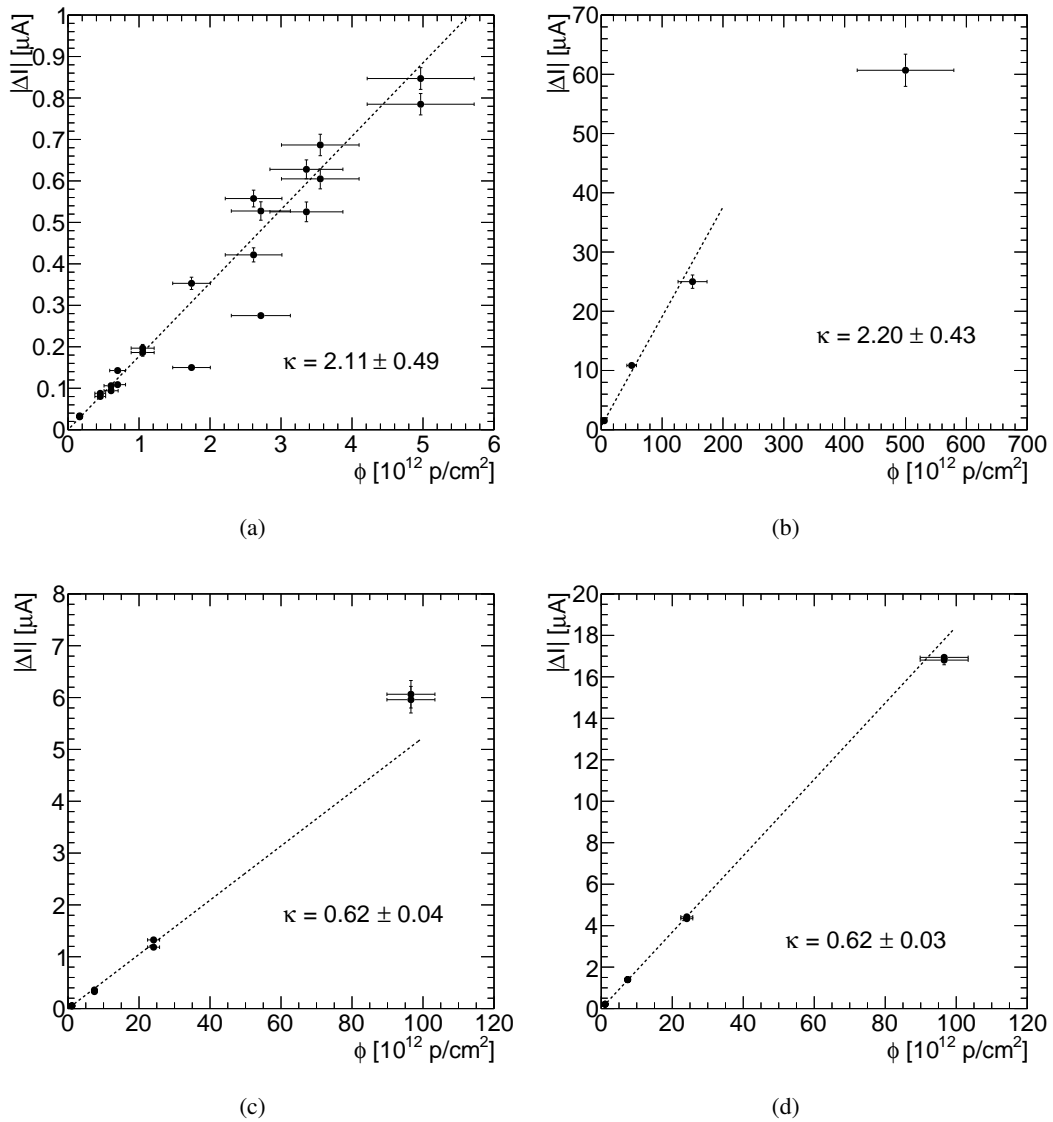
Figure 11. Change in leakage current as a function of proton fluence for BPW34F photodiodes irradiated at (a) the MC40 cyclotron; (b) the Irradiation Center Karlsruhe; and (c) at the IRRAD proton facility; (d) FZ pad diodes irradiated at the IRRAD proton facility.

In figure 12 the obtained measured values of the hardness factor are compared with the tabulated values found in the literature [9, 23, 24]. It is noted that the significantly larger uncertainties on the hardness factor for 23 and 24 MeV protons stems from uncertainties in the dosimetry, and, specifically, the uncertainty on the cross-section of the $^{28}Ni(p, X)^{28}Ni^{57}$ process which is taken conservatively to be approximately 20% based on the spread of cross-section measurements. Thanks to the higher proton energy, dosimetry at IRRAD is performed using aluminium foils, with the respective cross-setion uncertainty taken to be approximately 7% [25, 26]. As a result, these measurements could benefit from improved dosimetry, potentially through the use of a, specifically, designed, transmission ionisation chamber that could operate at large beam currents.
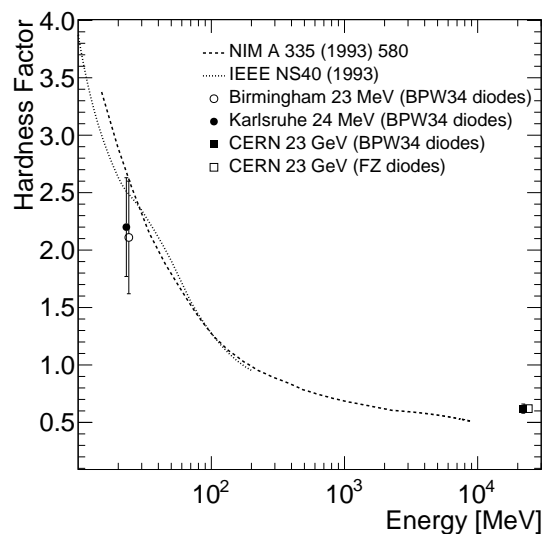
Figure 12. Measured proton hardness factors as a function of kinetic energy.

In the future, it is of interest to supplement this work with measurements at additional energies, for example the Cyclotron RadioIsotope Center (CYRIC) at Tohoku University [27] and the Los Alamos Neutron Science Center (LANSCE) facility [28] provide 70 and 800 MeV protons, respectively. Another development could involve other particle species, for example the PSI High Intensity Proton Accelerator (HIPA) provides irradiations with 300 MeV/c pions and the Jožef Stefan Institute TRIGA Mark II reactor [29, 30] provides irradiations with neutrons of a wide range of energies. An overview of the available irradiation facilities worldwide is provided by a CERN-maintained dedicated database [31].

5   Conclusions

By analysing the I–V and C–V characteristics of reverse biased BPW34F photodiodes pre- and post-irradiation, the hardness factors, κ, for three different proton energies were determined. Utilising the University of Birmingham MC40 cyclotron, a value of 2.1 ± 0.5 for an energy of 24 MeV was obtained. By undertaking a similar procedure, using the IRRAD proton facility, a value of 0.62 ± 0.04 for an energy of 23 GeV was measured. In parallel, the corresponding measurements with FZ pad diodes irradiated at IRRAD yielded a value of 0.62 ± 0.04. Using diodes irradiated at the Irradiation Center Karlsruhe, for an energy of 23 MeV, a value of 2.2 ± 0.4 was found. All measured values agree with the hardness factors currently in use at the facilities within one standard deviation. The measurements for 23 and 24 MeV protons have significantly larger uncertainties with respect to the 23 GeV measurement. The origin of this difference is in the dosimetry, which relies on nickel foils for 23 and 24 MeV protons, while aluminium foils are used for the 23 GeV protons. In the future, improved dosimetry could be achieved by using a transmission ionisation chamber, specifically designed for high rate operation.

Acknowledgments

References

[1] L. Evans and P. Bryant, *LHC Machine*, 2008 *JINST* **3** S08001.

[2] L. Rossi and O. Brüning, *Introduction to the HL-LHC Project*, *Adv. Ser. Direct. High Energy Phys.* **24** (2015) 1.

[3] ATLAS collaboration, *Letter of Intent for the Phase-II Upgrade of the ATLAS Experiment*, CERN-LHCC-2012-022 (2012).

[4] CMS collaboration, *Technical Proposal for the Phase-II Upgrade of the CMS Detector*, CERN-LHCC-2015-010 (2015).

[5] P. Dervan et al., *Upgrade to the Birmingham Irradiation Facility*, *Nucl. Instrum. Meth.* **A 796** (2015) 80.

[6] A. Dierlamm, *Proton irradiation in Karlsruhe*, at *16th RD50 — Workshop on Radiation hard semiconductor devices for very high luminosity colliders*, Barcelona Spain (2010).

[7] M. Moll, E. Fretwurst, G. Lindström and M. Kuhnke, *Relation between microscopic defects and macroscopic changes in silicon detector properties after hadron irradiation*, *Nucl. Instrum. Meth.* **B 186** (2002) 100.

[8] RD50 collaboration, http://rd50.web.cern.ch/rd50/.

[9] M. Huhtinen and P.A. Aarnio, *Pion induced displacement damage in silicon devices*, *Nucl. Instrum. Meth.* **A 335** (1993) 580.

[10] P. Allport et al., *Recent results and experience with the Birmingham MC40 irradiation facility*, 2017 *JINST* **12** C03075.

[11] GEANT4 collaboration, *GEANT4: A Simulation toolkit*, *Nucl. Instrum. Meth.* **A 506** (2003) 250.

[12] J. Allison et al., *Recent developments in Geant4*, *Nucl. Instrum. Meth.* **A 835** (2016) 186.

[13] D. Cundy and S. Gilardoni, *The Proton Synchrotron (PS): At the Core of the CERN Accelerators*, *Adv. Ser. Direct. High Energy Phys.* **27** (2017) 39.

[14] V. Cindro, *World Irradiation Facilities for Silicon Detectors*, PoS(Vertex2014)026.

[15] B. Gkotse, M. Glaser, M. Moll and F. Ravotti, *IRRAD: The New 24 GeV/c Proton Irradiation Facility at CERN*, in *Proceedings of 12th International Topical Meeting on Nuclear Applications of Accelerators (AccApp 2015)*, Washington D.C. U.S.A. (2015), pg. 182.

[16] Irradiation Center Karlsruhe, Institute of Experimental Particle Physics, KIT, http://www.etp.kit.edu/english/irradiation_center.php.

[17] ZAG Zyklotron AG, http://www.zyklotron-ag.de/en/.

[18] A. Chilingarov, *Temperature dependence of the current generated in si bulk*, 2013 *JINST* **8** P10003.

[19] M. Moll, *Radiation damage in silicon particle detectors: Microscopic defects and macroscopic properties*, Ph.D. Thesis, Hamburg University, Hamburg Germany (1999).

[20] OSRAM Opto-Semiconductors, *Bpw34 silicon pin photodiode datasheet*, available online from http://www.osram-os.com.

[21] F. Ravotti, M. Glaser and M. Moll, *Sensor catalogue data compilation of solid-state sensors for radiation monitoring*, CERN-TS-Note-2005-002 (2005).

[22] F. Ravotti, M. Glaser, M. Moll and F. Saigne, *BPW34 Commercial p-i-n Diodes for High-Level 1-MeV Neutron Equivalent Fluence Monitoring*, *IEEE Trans. Nucl. Sci.* **55** (2008) 2133.

[23] A. Vasilescu and G. Lindstroem, *Displacement damage in silicon, on-line compilation*, https://rd50.web.cern.ch/rd50/NIEL/.

[24] G.P. Summers et al., *Damage correlations in semiconductors exposed to gamma, electron and proton radiations*, *IEEE Trans. Nucl. Sci.* **40** (1993) 1372.

[25] A. Curioni et al., *Single- and multi-foils $^{27}Al(p,3pn)$ ^{24}Na activation technique for monitoring the intensity of high-energy beams*, *Nucl. Instrum. Meth.* **A 858** (2017) 101.

[26] M. Glaser, F. Ravotti and M. Moll, *Dosimetry assessments in the irradiation facilities at the CERN-PS accelerator*, *IEEE Trans. Nucl. Sci.* **53** (2006) 2016.

[27] K. Nakamura et al., *Irradiation and testbeam of KEK/HPK planar p-type pixel modules for HL-LHC*, 2015 *JINST* **10** C06008.

[28] K.F. Schoenberg and P.W. Lisowski, *LANSCE:A Key Facility for National Science and Defense*, *Los Alamos Science* **30** (2006) 2.

[29] S. Aghara and W. Charlton, *Characterization and quantification of an in-core neutron irradiation facility at a triga ii research reactor*, *Nucl. Instrum. Meth.* **B 248** (2006) 181.

[30] L. Snoj, G. Žerovnik and A. Trkov, *Computational analysis of irradiation facilities at the JSI TRIGA reactor*, *Appl. Radiat. Isot.* **70** (2012) 483.

[31] http://irradiation-facilities.web.cern.ch/.